Int J Fract (2009) 159:51–62
DOI 10.1007/s10704-009-9382-z

ORIGINAL PAPER

Experimental observation of fracture patterns in layered slate

B. Debecker · A. Vervoort

Received: 14 April 2009 / Accepted: 9 July 2009 / Published online: 1 August 2009

Abstract The layered structure of slate rock induces strength anisotropy. The strength in the direction of the layers (schistosity) is considerably smaller than in any other direction. A series of loading tests on circular samples and another series of loading tests on rectangular samples are performed to examine fracture patterns in slate. The tests are monitored by visual recordings and by recording acoustic emission. The processing of this data results in localization. This allows identification and analysis of the occurrence and propagation of the individual fractures. It is shown that the strength anisotropy on μ-scale is the key factor behind the strength anisotropy on sample scale, as well as behind the deformation behaviour of the sample. In addition, it is observed that a small variability in the layer direction can affect the fracture pattern considerably.

Keywords Rock mechanics · Fractures · Strength anisotropy · Brazilian test · Digital image processing

Abbreviation

AE Acoustic emission

B. Debecker (✉) · A. Vervoort
Department of Civil Engineering, Catholic University of Leuven, Kasteelpark Arenberg 40, bus 2448, Leuven 3001, Belgium
e-mail: bjorn.debecker@bwk.kuleuven.be

1 Introduction

In rock, as in any other brittle material, when stresses become sufficiently large, fractures start to appear. Depending on the properties of the rock, the resulting fracture pattern can evolve at constant or increasing deformation level. Next to the strength properties of rock, the actual deformation behavior is important too for engineering applications. The surface under the strain-deformation curve is a measure for how much energy a rock can absorb before and after failure. Pure brittle behavior results in a complete loss of strength once the peak strength is reached (Andreev 1995), while on the contrary other rock types can have a considerable amount of post-peak strength, allowing additional deformation with very little or no loss of strength. The behavior of slate is, among others, important in oil drilling context. Slate or its less metamorphic variant, shale can be found as cap rock on top of hydrocarbon reservoirs (Al-Bazali et al. 2005) or in fractured state as reservoir rock (Sircar 2004). Borehole instability in oil and gas drillings results every year in considerable financial losses during exploration and production.

If a rock is isotropic, the overall direction of fractures is generally only influenced by the stress orientation within the rock. Slate however, is a layered rock that is at its weakest along its layer direction, also called schistosity. This causes the fracture pattern in slate to be dependent also on the anisotropic rock mechanical parameters. Fractures can grow parallel to the weaker layers, or in other directions, or as a combination of

Table 1 Overview of all circular samples (1st series)

Angle θ (°)	0	5	10	15	20	25	30	45	50	60	70	80	90
Samples	A1	B3	B5	B7	B9	B14	B15	B16	A2	A7	A8	A9	A10
	B1	B4	B6	B8	B13					B17			
	B2	B10	B11	B12									

Diameter and thickness are respectively, 100 and 40 mm for the A-samples and 80 and 30 mm for the B-samples

both. To analyze or predict fracture patterns in such a rock, a good knowledge on stress conditions and rock mechanical parameters in both layer direction and in the other directions is required.

In this study, two series of rock mechanical loading tests on slate are performed. The two types of tests, namely the diametrically loading tests on the circular samples, called a Brazilian test (to induce tensile stresses) and the uniaxial compressive loading tests on the rectangular samples each induce a different stress state within the sample. During the tests, the origin and evolution of fractures are digitally monitored by acoustic and/or visual techniques. First, the tests on the circular samples are conducted to focus on the influence of schistosity orientation relative to the loading direction, on the 2D-fracture pattern. Second, the uniaxial loading tests examine the fracture pattern for a fixed configuration in order to identify different properties and relate this to strength and deformation behavior. Additionally, it is evaluated if a 2D-aproximation of the fracture patterns suffice for thin samples, supported by 3D-localisation through acoustic emission (AE).

This study is part of a larger research where the experimental results are also used as data for the validation of numerical simulations of the fracturing of layered rock (Debecker and Vervoort 2009a).

2 Experimental set-up

The slate in this study comes from a quarry in Herbeumont, Belgium and consists almost entirely of quartz, sericite, chlorite and cubic pyrite inclusions. Slate is derived from low grade metamorphose of sedimentary shale. To be more precise, it is actually a phyllite, i.e. a gradation in the degree of metamorphism between slate and mica schist. The slate has a fine and homogeneous structure and a very low porosity with a value of 0.016 (De Barquin and Nicaise 2005). Through realignment of platy mica crystals, orthogonal to the maximum principal stress direction, the slate exists as a sequence of many parallel planes, called the schistosity planes. Along the schistosity planes, both tensile strength and shear strength of the rock are at their weakest. Two series of samples are prepared from the slate rock. A first series of 23 circular samples consists of two types: one type has a diameter and a thickness of respectively, 100 and 40 mm (A1–A2, A7–A10), a second type measures respectively, 80 mm and 30 mm for diameter and thickness (B1 to B17). The loading of circular samples is used to induce tensile stresses and is often called a Brazilian test. In a classical Brazilian tensile test, a circular disc is loaded in compression on two opposite lines. In isotropic rock, tensile stresses are induced along the plane of loading due to elastic relaxation of the sample in the direction orthogonal to the loading lines. Note that in this anisotropic layered rock, on μ-scale (i.e. in between two schistosity layers) there are only two strength values assumed, namely one μ-scale strength value along the layer direction and one μ-scale strength value for all other directions. The fracture pattern and overall strength of the slate in such a test is determined predominantly by the μ-scale strength in the schistosity direction or the μ-scale strength in the other directions, or a combination of both. As the angle between the schistosity direction and the loading plane varies, the predominant property changes, and thus the fracture pattern and the overall strength. θ is defined as the inclination angle between the loading direction and the normal to the schistosity direction. This angle varies in this series of tests from 0° to 90° as summarized in Table 1.

The second series consists of five rectangular samples (C1 to C5) with a width and a height of respectively, 60 and 130 mm and a thickness of 29 mm (Table 2). The samples are compressed parallel to the height. For this series of tests, the angle θ between the

Table 2 Overview of all rectangular samples (2nd series)

All C-samples have the following dimensions: 130 mm(height) × 60 mm (width) × 29 mm (thickness)

Angle θ (°)	20
Samples	C1
	C2
	C3
	C4
	C5

loading direction and the normal to the schistosity is constant at a value of 20°. Contrary to the loading tests on the circular samples, where the rock fails in tension, under uniaxial compressive load the rock fails in shear or as a combination of shear and tensile failure. While tensile stress in rock occurs mainly around excavations due to stress redistribution (Ewy and Cook 1990), compressive stress in rock prevails in natural conditions (Brady and Brown 1993).

Since the thickness is considerably smaller than the other dimensions for all samples, the intention is to study the fractures as 2D-features under these configurations. For all samples, the angle with the circular surfaces studied is $90° \pm 2°$ (due to sample preparation accuracy and natural variability). All the samples are loaded displacement controlled. The tests on the rectangular samples do not stop at the maximum load, but continue as the samples are able to support a reduced load in the post peak stage.

The circular test samples (first series) are loaded at a rate of 0.1 mm/min. All uniaxially loaded samples (second series) are loaded initially at a rate of 0.5 mm/min until a given load level (80 kN for B1, 50 kN for all other samples) at which the loading rate is decreased to 0.05 mm/min. These loading rates are much smaller than conventionally in order to better observe the evolution of the fracture patterns.

The samples are tested as shown in Fig. 1. In front of the load frame, a digital camera is mounted to monitor visually the fractures on one sample surface. In an earlier attempt, a digital photo camera was used. However, for the tests discussed here, it is replaced by a video camera. The advantage of a video camera is that it generates a continuous sequence of pictures at high rate. In this case, the recorded movie consists of 25 frames per second, thus one picture every 40 ms. The disadvantage is the reduced resolution: a frame of a video movie has a resolution of 0.3 Mpix, while a modern digital photo camera has a resolution of 10 to

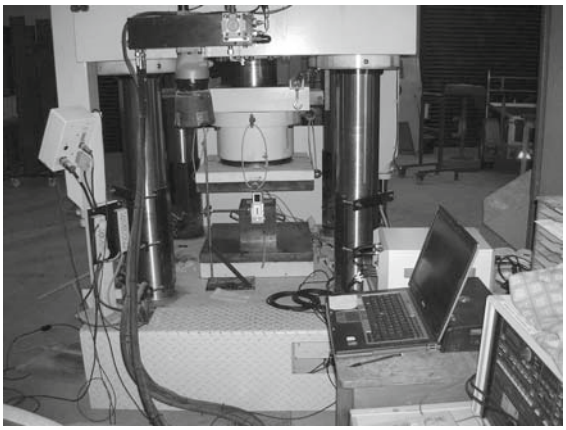

Fig. 1 Experimental set-up. The sample is placed under the loading frame (*central*) and monitored both by a digital camera, as well as AE equipment (*box* in *front, right*)

15 Mpix. High resolution is a requisite for e.g. strain registration, where small deformations are examined by pixel comparison of sequential pictures (Lomov et al. 2006). However, in this study, a high picture rate was preferable to high resolution, as is illustrated later on.

For the video observation, larger diameters do not result in better images, since the resolution of the video images is restricted to 720 × 576 pixels, regardless of the sample size. However, with increasing dimensions there is an increasing probability of cutting through an open schistositiy layer during sample preparation, resulting in a broken sample. That is why the circular discs are decreased in diameter from 100 mm (A-samples) to 80 mm (B-samples).

In addition, the second series of tests is also monitored by means of acoustic emission (AE) equipment. Micro cracks that develop in rock or in other material generate elastic strain waves that can be recorded by AE sensors. Two wide-band sensors are positioned on the front surface (i.e. the surface filmed) and two on the rear surface. Similar to GPS positioning, the exact position of such a micro crack can be determined by triangulation. The arrival of one signal is recorded (and called a 'hit') at different times for different sensors, depending on their distance to the origin of the signal. By multiplying these arrival time differences by the wave velocity, the difference in distances from the signal source to each of both sensors can be calculated for any pair of sensors. Hence, if a sufficient number of sensors record the signal, the exact position of the

signal source (i.e. micro crack) can be calculated, a technique referred to as 'localization' (Grosse et al. 2003). Thus, this technique can provide information related to fracturing from the interior of the sample, contrary to visual observations that are restricted to the outside surfaces during testing. For 3D localization, a theoretical minimum of four sensors is required to record the signal. An additional difficulty with slate, is that the wave velocity in slate is not isotropic, but direction dependent. The different velocities are experimentally measured and a program is written in Matlab to perform localization (Debecker and Vervoort 2009b).

3 Results from the loading tests of the circular samples

The maximum load for each test is recorded. In order to compare the peak stress in the circular samples with different dimensions and/or different inclination angles, the peak stress parameter Ψ is defined as:

$$\psi = \frac{2F}{\pi Dt} \tag{1}$$

where F is the maximum load applied, D the sample diameter and t the sample thickness. If a rock material is isotropic and the deformation occurs elastically, Ψ is equal to the tensile strength, and the test is referred to as the Brazilian tensile test (Jaeger and Cook 1976). Since slate is anisotropic and the fracture pattern is often a combination of failure in tensile mode and in shear mode, Ψ does not equal the tensile strength in this study. To find the stress distribution within the sample at the time of failure and to determine the failure mode(s), numerical simulations have to be performed. The fracture mechanisms in slate are therefore further studied by discrete element modeling (Debecker and Vervoort 2009a).

In Fig. 2, the peak stress is presented in function of the angle between the loading direction and the normal to the schistosity, θ. The peak stress is maximal (20.0 MPa) when the loading direction is orthogonal to the schistosity ($\theta = 0°$) and decreases rapidly for increasing values of θ. In the interval between 45° and 90° for θ, the peak stress becomes minimal and nearly constant at a value of 0.4 ± 0.1 MPa. For the samples with θ larger than 30°, there is a clear maximal load peak, followed by a nearly complete loss of strength thereafter. However, for the samples with inclination

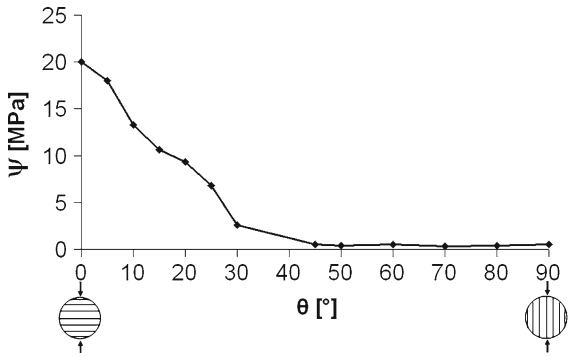

Fig. 2 Peak stress Ψ in function of the inclination angle between loading direction and normal to the schistosity direction, θ

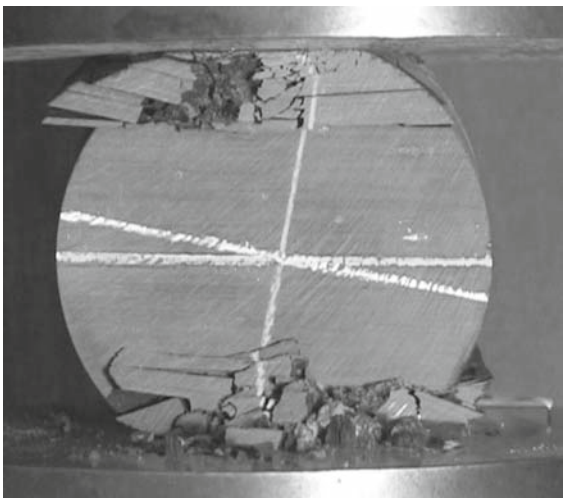

Fig. 3 Sample B12 ($\theta = 10°$) at the end of testing. *Top side* and *bottom* are crushed

angles smaller than 30°, there is no distinctive maximum on the load curve. It is observed that for these samples at a certain load, fracturing becomes very intensive at the top side and at the bottom of the sample. In these regions, the rock loses consistency and small pieces are chopped of, resulting in a flattening of the disc as can be seen in Fig. 3. Thus, the contact surfaces increase, and consequently the force that can be supported by the sample. At this time, Formula (1) is obviously no longer valid as the peak stress within the circular sample. Therefore, the peak stress values in Fig. 2 for angles up to 30° are calculated with the maximal load before the onset of the sample crushing (e.g. "6" on Fig. 6; see further). This data serves mainly to compare the strength for different values of θ, and not as a determination of tensile strength values as such.

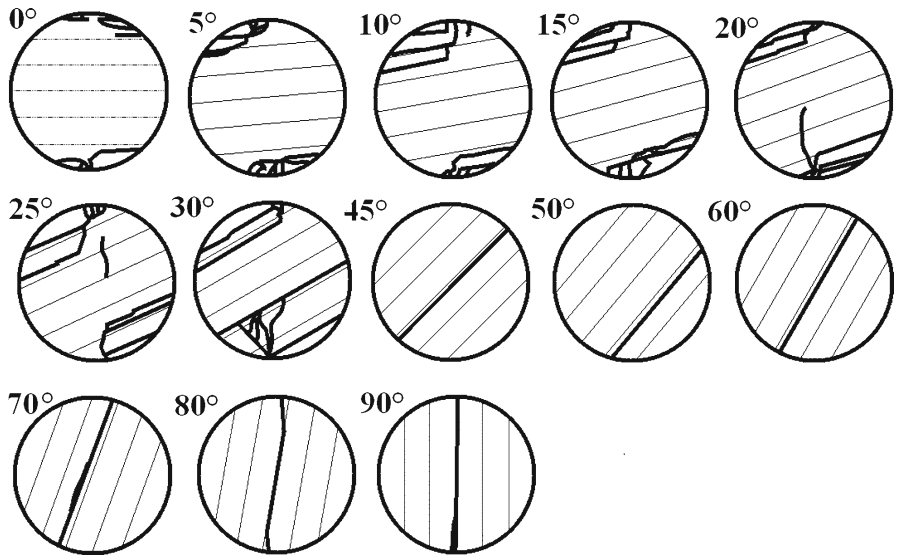

Fig. 4 Fracture patterns after Brazilian tensile testing, for samples with increasing angle θ. The parallel thin *lines* indicate the schistosity direction. Presented samples with $\theta \leq 45°$ have Ø 80 mm, those with $\theta > 45°$, Ø 100 mm

Next, the final fracture patterns after testing are digitalized and presented in Fig. 4. Note that for each value of θ, only one, but representative fracture pattern is shown, in order not to lose the overview. First, for all samples, fractures in the direction of the schistosity are observed. Second, fractures in other directions are observed only for samples with θ between 0° en 30°. In this same range, fractures occur more centrally as θ increases. Third, for all samples with θ larger than 30°, the fracture pattern is restricted to one fracture in the schistosity direction, going from one end of the sample to the other. Only for θ equal to 80° and 90° does this fracture start at one loading line and end at the other one.

The transition from mixed mode fracturing (i.e. fractures in the schistosity direction and fractures in other directions) to fracturing only in the schistosity direction occurs thus for θ between 30° and 45°. This corresponds well to the transition in peak stress as seen on Fig. 2 and discussed above. It is believed that for angles up to 30°, the overall strength is dependent both on μ-scale strength in the schistosity direction and on μ-scale strength in the other directions. As θ increases, the μ-scale strength in the schistosity direction, which is the weakest, becomes more dominant and thus the overall strength decreases. For angles larger than 30°, the strength is believed to be mainly determined by the μ-scale strength in the schistosity direction and thus becomes almost independent of θ. Although it seems by these observations that shear failure occurs along a schistosity plane, it is possible that on μ-scale there is actually a mixed mode of failure (i.e. shear and tensile failure). Numerical simulations can provide further insight in this. In addition, inter-layer cracks on μ-scale may be undetected by this observation technique, given that the thickness of the schistosity layers is in the order of magnitude of 100 nm.

Tavallali et al. (2007) observed a similar transition from mixed mode fracturing to (dominantly) fracturing in schistosity direction in layered sandstone for θ between 45° and 60°.

Finally, it is also possible to study the evolution of the fracture pattern. By comparing sequential snapshots of the video stream (so-called frames), one can determine the occurrence of different fractures and their direction of propagation (Fig. 5). This can be done because the time interval between two successive frames (40 ms) is most of the time sufficiently small to see the fracture propagates. This determines the choice for video imaging since the corresponding rate of images (25 per second) cannot be obtained during the entire test when working with a photo camera. In addition, the occurrence of different fractures can be linked to the load versus time–graph.

The evolution of the fracture pattern is discussed below for one specific test as a representative example.

Figure 6 presents the load versus time curve for sample B14, which has an angle θ of 20°. The different separate fractures are indicated on the enclosed drawings. The following observations are made:

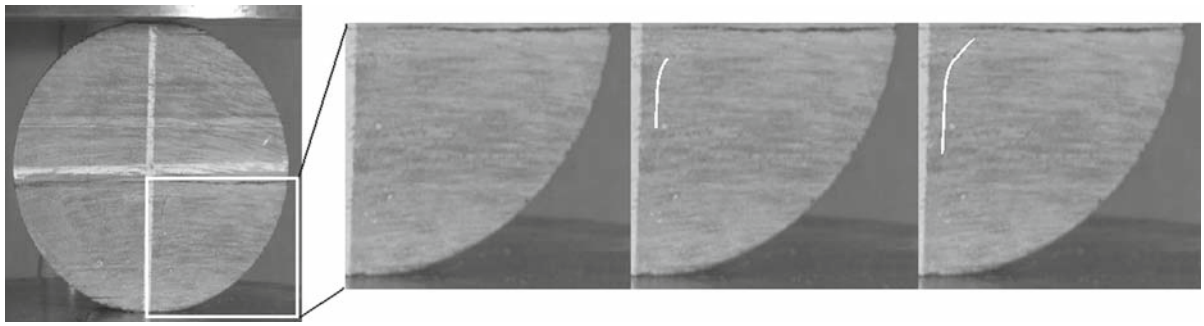

Fig. 5 Growth of a fracture as observed in slate sample B1 ($\theta = 0°$) (*left*). Three sequential magnifications (*right*) show an identical part of the sample but with a time interval of 40 ms between two successive images. The fracture is colored *white* for illustrative purpose

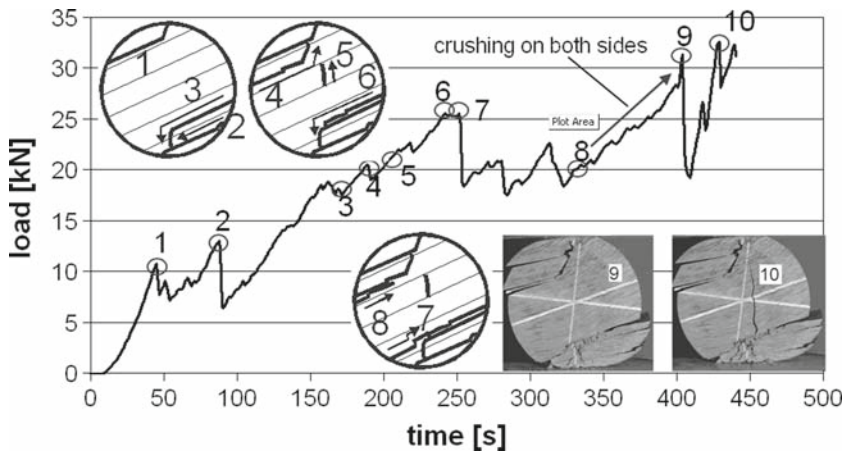

Fig. 6 Load versus time graph for sample B14 ($\theta = 20°$). The drawings show the propagation of different fractures at corresponding load peaks

- Most fractures are initially in the direction of schistosity and deviate in another direction after the fracture has propagated over a certain length. The fractures grow from the edge of the sample towards the interior. In a few cases, the propagation is too fast to determine the direction of propagation and only the resulting fracture can be observed (e.g. fracture 1).
- The first fractures are situated near the loading lines, i.e. on top and in the bottom of the sample (e.g. fractures 1, 2, 3). This is because large stress concentrations are induced in the regions around the loading lines. After this, new fractures originate closer to the centre of the sample (e.g. fractures 4, 6).
- Fractures that do not follow the schistosity direction anywhere over its entire length (e.g. fracture 5) are rather rare in the entire series of tests. This type of fractures resembles the tensile fractures, known from Brazilian tests on isotropic material (Andreev 1995; Van de Steen et al. 2005).
- The occurrence of new fractures can be clearly observed on the load curve by corresponding local load drops, as indicated by circles on this curve. On the other hand, not every load drop could be correlated to the visual observation of a new fracture. This is probably because these load drops are caused by fractures on a smaller scale, which can not be observed on the pictures.

Most observations here are valid for all tests with θ up to 30°. In all these tests, the crushing, as described above, is observed. Most of these tests are manually stopped after this crushing had become too extensive. However, a few samples lost strength after the occurrence of a subvertical, diametrical fracture as can be seen on Fig. 6 (fracture 10).

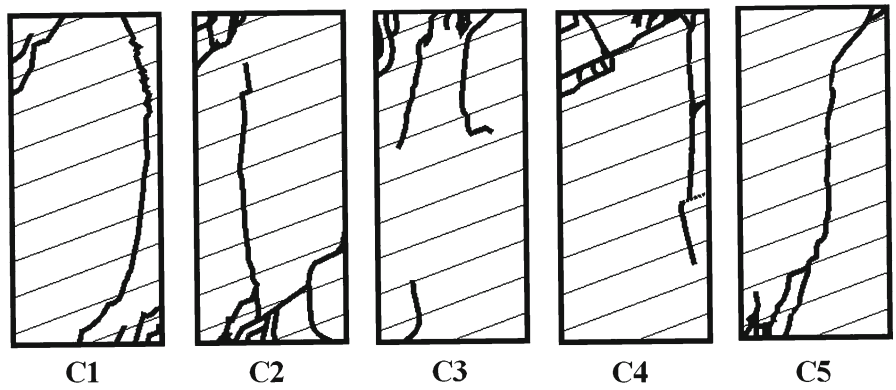

Fig. 7 Fracture patterns after testing, for 5 samples with $\theta = 20°$. The parallel thin *lines* indicate the schistosity direction. All samples measure 60 mm × 130 mm

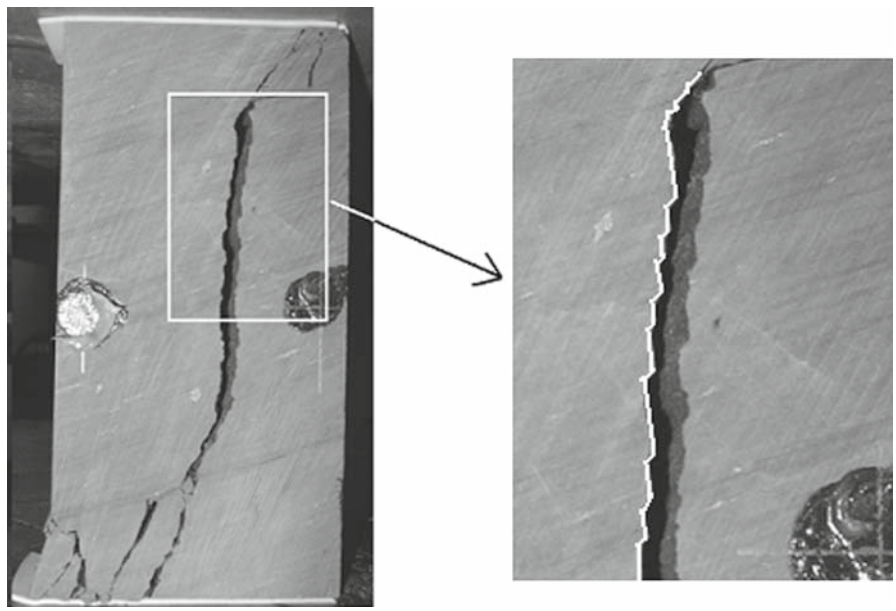

Fig. 8 Sample C5: fracture after testing (*left*) and magnification (*right*) where the 'en echelon'-like fracture is indicated by the *white line*

4 Uniaxial loading test results

In the previous test, the most 'interesting' fracture patterns (i.e. consisting of fractures in different directions) are observed for inclinations between horizontal and 30°. Therefore, in this new series an inclination angle of 20° is chosen.

All samples have reached a maximum load between 44 and 52 MPa, except for C5 with a maximum of only 25 MPa. The compressive strength in these tests is thus around 5 times larger than the peak stress for a circular sample with θ equal to 20°. Note that the uniaxial strength in this study is not according to the ISRM standards, which prescribes the use of cylindrical samples with a height to diameter radius of 2.5–3.0 (ISRM 1979). However, for a good 2D visualization, it is better to work with flat surfaces, instead of cylindrical surfaces, hence the choice for rectangular shapes rather than cylindrical samples.

Figure 7 presents the fracture patterns after testing, observed on the surface that is filmed. It is clear that the fracture patterns consist of fractures along the schistosity direction and subvertical fractures. However, often a subvertical macro fracture is in fact a combination of small vertical fractures combined with small fractures in the schistosity direction (Fig. 8), and resembles a fracture made up of 'en-echelon' flaws as described by Bombolakis (1968). The en-echelon structure is observed in other rock materials as well, e.g. in granite where cleavage planes define the form (Friedman et al.

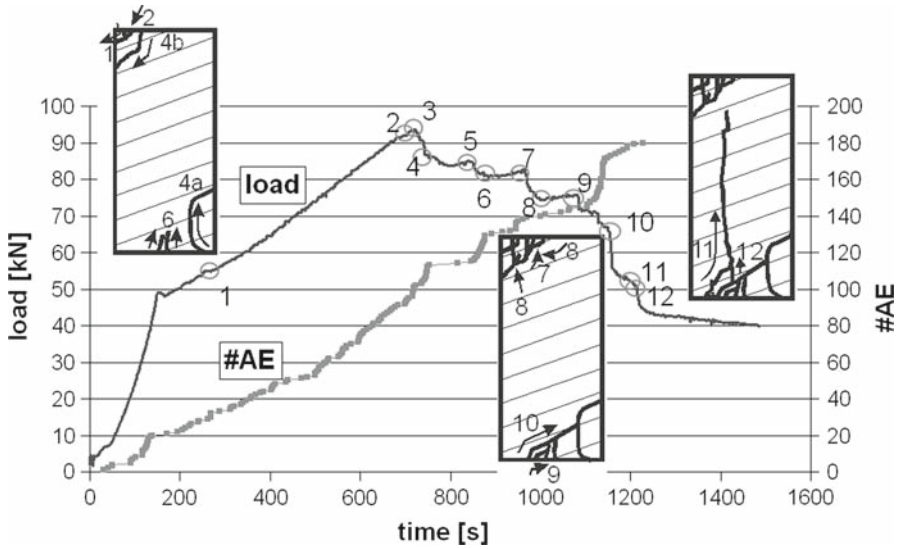

Fig. 9 Sample C2. Load vs. time (*left axis*) and cumulative number of AE-hits vs. time (*right axis*). The *circles* indicate events that can be determined on the load-time *curve*. The *circles* correspond to the observations of fractures

1970) or in quartzite and chlorite schists (Nasseri et al. 1997).

Similar to the tests with the circular samples, the video images provide the possibility to examine the occurrence and propagation of individual fractures. Figure 9 illustrates the load versus time graph of sample C2 (left axis) and the cumulative number of AE-hits versus time (right axis), together with the schematic drawings of the fractures observed on the front surface.

- The first fractures appear in the bottom part or the top part of the sample, in a (sub)vertical direction. These cracks then deviate in the direction parallel to the schistosity (e.g. fractures 1 and 4a). Alternatively the fracture can start parallel to the schistosity and then deviate towards the subvertical direction (e.g. fracture 10).
- After the peak load is reached, a sub vertical fracture going from top to bottom occurs (fracture 11). This is also observed for C1 and C5 (Fig. 7), but not in C3 or C4.
- Again, the occurrence of new fractures can be related well to the load curve by corresponding local load drops, as indicated.
- A considerable post peak-strength is observed in all samples. Energy dissipation occurs during both pre- and post-peak through (local) shear fractures along the schistosity planes and interconnecting tensile cracks, thus preventing an explosive behavior at peak stress level. This mechanism corresponds to the crushing of the circular sample tests that prevented an overall failure of the sample and allowed it to support increasing load.

In addition, the cumulative number of AE-hits versus time is drawn (right axis). Only the hits that are recorded by all four sensors are presented, since localization of a hit can only be performed if the hit is recorded by four sensors. It can be seen that this curve follows quite well the trend of the load curve. This means that the occurrence of fractures corresponds to increased AE activity. In the post-peak stage, both curves move evidently in the opposite direction because the load decreases gradually while the total number of recorded hits is further increasing.

Finally, the AE data is used for localization. The exact set-up and method of calculation is described by Debecker and Vervoort (2009b). Figure 10 presents the different stages of fracture growth that are visually observed, referred to by the same numbers, together with the positions of the localized acoustic events, for sample C2. All hits are projected on the xy-plane, the largest plane of the sample (parallel to the surface that is visually monitored). In pre-peak stage, the localized hits are situated all over the sample. In the post-peak stage, starting with fracture 4b, the hits are localized in the same zone as the visual observations of the fracture (i.e. 4b: upper zone, 6: lower zone, 7–8: upper zone, 9-10: lower zone, 11-12: lower zone).

Since the localization is performed in 3D, also a lateral projection (i.e. in the direction of thickness) of

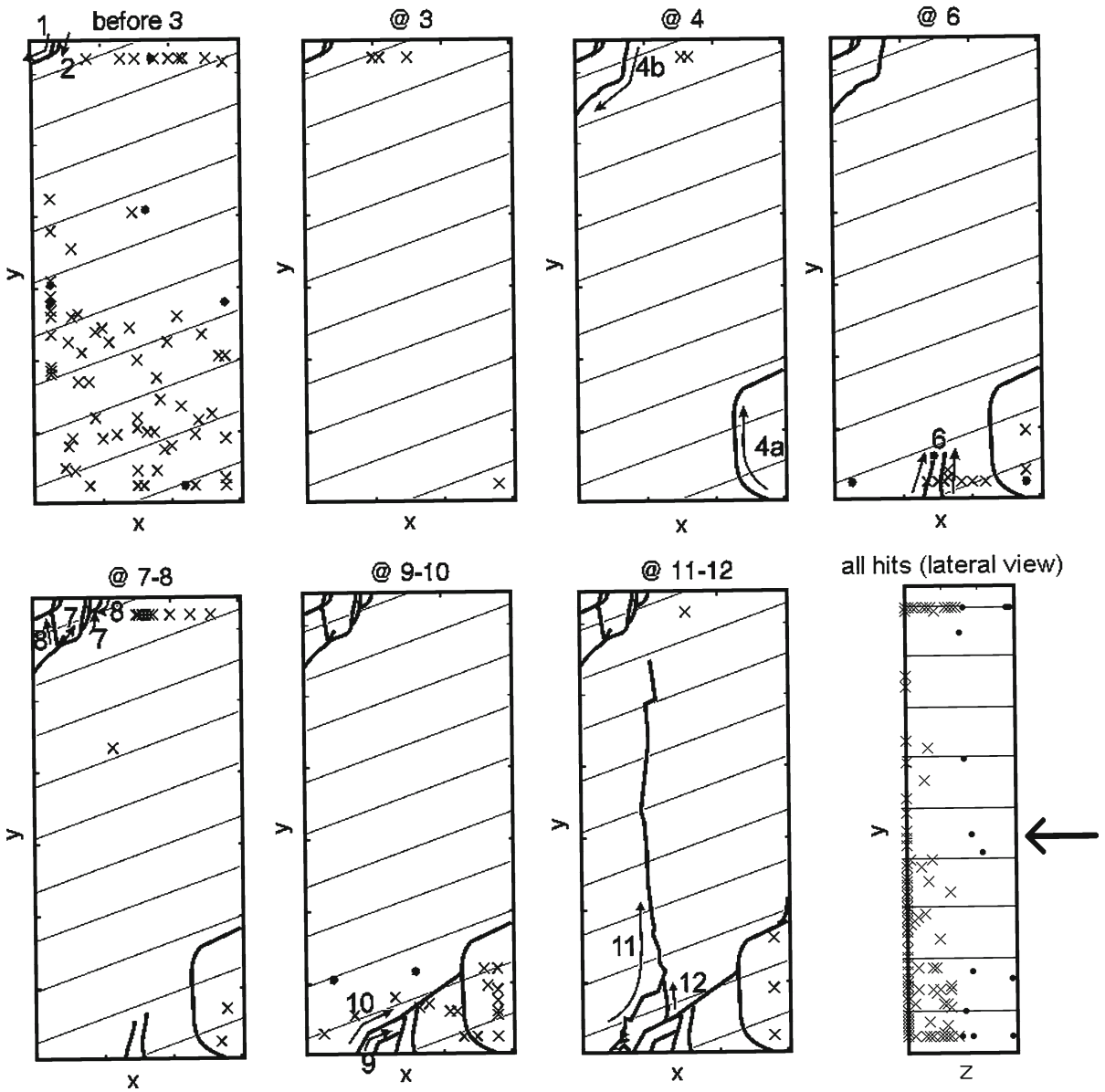

Fig. 10 Slate sample C2. The occurrence of new fractures during different phases as observed on Fig. 9. *Crosses* and *dots* are hits localized during these phases, respectively, in the rear half or in the front half of the sample. The last drawing is a lateral view of all localized hits. The *arrow* indicates the filmed surface

the positions of the hits can be made (see bottom, right in Fig. 10). This shows that most hits are not localized on the surface that is visually observed (indicate by the arrow). Many hits appear within the interior of the sample or on the rear surface or the rear part of the sample, i.e. further away from the surface that is filmed. The scattered AE activity in the interior of the sample is an indication for the 3D-character of the fractures. Initially it was thought that fractures in these samples (i.e. with a relatively small thickness) could be regarded as roughly planar. This implies that for all interior planes parallel to the exterior (filmed) surface, the fracture pattern should look roughly the same. However, by comparing the front and rear surface of

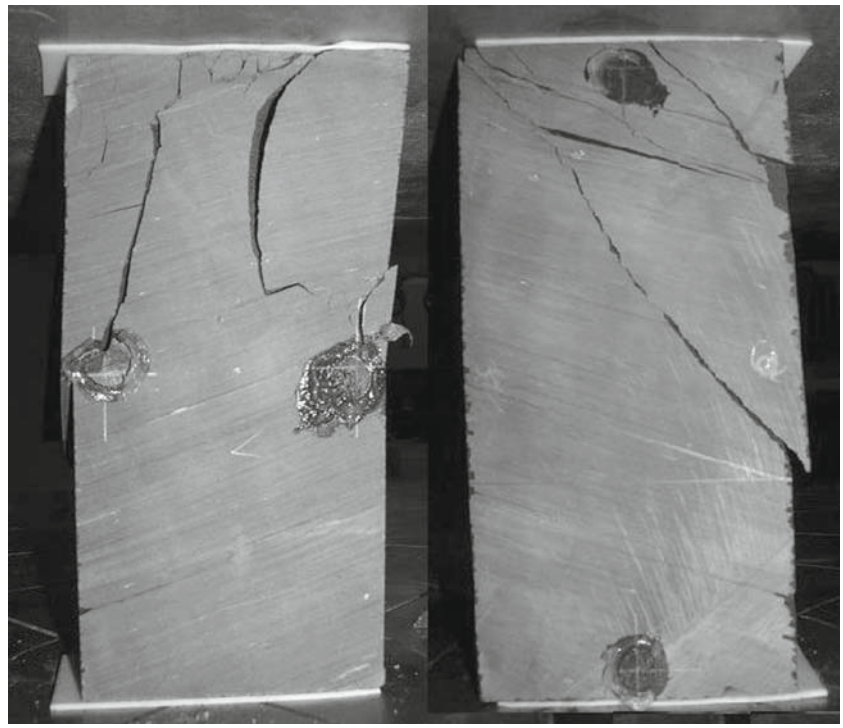

Fig. 11 Slate sample C3: Fracture pattern after testing: front (*left*) and rear (*right*). Fracture patterns are considerably different on both sides of the sample

the tested samples, it is observed that the fracture patterns differ considerably in some cases as can be seen most clearly in sample C3 on Fig. 11. The reason for this is most likely the small degree of imperfection in the arrangement of the schistosity planes. The actual orientation of the schistosity planes is not completely constant and can locally vary by some degrees. This can cause fractures to cross from one schistosity plane to another within the sample, not necessarily at the same positions as seen on the outside surface, resulting in an irregular, 3D fracture pattern. In addition, this slight variability in schistosity orientation makes it also difficult to prepare samples in which the schistosity planes are orthogonal to the front surface. The resulting error of margin from sample preparation might thus add up to the above described effect.

Next to this, small micro cracks (nm-scale) are present in slate already before testing, due to the stress history and the geological metamorphosis (Abad et al. 2003). These micro cracks are typically parallel to the schistosity and are scattered across the sample. When a sample is loaded, they can extend further and induce AE activity.

Finally, it is observed that sometimes a pyrite inclusion can serve both as a nucleus or a hindrance for fracture growth (Fig. 12).

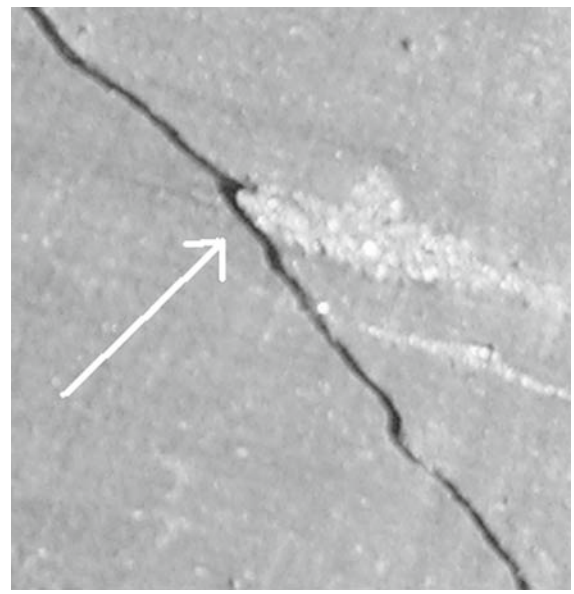

Fig. 12 Detail from slate sample C1 where the fracture deviates due to the hindrance of a pyrite inclusion (*arrow*)

5 Discussion on fracture mechanisms and their importance

Given its structure, the predominance of a fracture mode, namely axial tensile fractures or shear fracturing

along the schistosity, is among others, highly dependent on the relative orientation of schistosity to the applied stress direction. Jaeger (1960) presented a simplified model for failure of a layered rock under uniaxial compressive load (comparable to the tests on rectangular samples discussed here). According to his theory, the rock fails in shear along the schistosity if θ is larger than the friction angle of the schistosity layers, ϕ. For smaller values of θ, the rock fails with the occurrence of subvertical axial tensile fractures, or of shear fractures at an angle different from θ, and the strength is assumed independent of θ within this range. However, the uniaxial compressive tests where θ is 20° show that both sub vertical tensile fractures and shear fractures in schistosity direction occur (Fig. 7). The latter contradicts partially Jaeger's theory that predicts shear fractures at an angle different from θ. Similar observations are made for the tests on the circular samples with θ smaller than 45° (Fig. 4). Thus, the strength of a sample on macro-scale (i.e. sample scale) in a given direction can be dependent on a combination of μ-scale strength in different directions.

Wawersik and Fairhurst (1970) determined two types of post peak behavior for brittle rocks under compressive stress. On the one hand they define a type I, where fracture propagation is stable, and thus incremental displacement must be imposed for incremental decrease in strength. On the other hand, there is type II for which the fracture evolution is unstable or self-sustaining. They also determine two different modes of fracture, namely local axial tensile fractures (parallel to the applied load) and local and macroscopic shear fracture (faulting). Furthermore they state that for very homogenous materials axial fracturing does not occur since the absence of heterogeneities prevents local stress concentrations large enough for local tensile fractures. Contrary to this, in very heterogeneous rock, local axial failure is too dominant for shearing to occur. Van de Steen et al. (2002) also showed that an increase in the amount of heterogeneity resulted in a decrease of tensile strength for crinoidal limestone.

It becomes clear that the layered slate in this study can only be fitted partially within the theory above. The subvertical fractures observed in these tests are believed to be tensile fractures. The fractures in schistosity direction are generally in shear mode, unless their orientation coincides roughly with the loading direction, they are assumed to be in tensile mode (e.g. test on circular samples with θ equal to 80° or 90°). While slate is anisotropic, namely transversely isotropic, it is at the same time rather homogenous. The latter implies that its composition is uniform, throughout its volume. The heterogeneities in the sample are small cubic pyrite inclusions. Both tensile and shear fractures are observed within the tests discussed in this paper. But here, the shear fractures are mainly due to the lower shear strength in the schistosity direction, and not due to the absence of multiple heterogeneities as described by Wawersik and Fairhurst (1970). Energy dissipation occurs during both pre- and post-peak stage through (local) shearing along the schistosity planes and interconnecting tensile cracking, thus preventing an explosive behaviour at peak stress level. Having a pronounced elongated post-peak behavior, the slate could be designated as type I in Wawersik and Fairhurst's classification. However, instead of 'brittle', on macro-scale the slate behaves rather 'ductile', meaning that it can sustain further deformation without losing much load-carrying capacity. Thus the evident difference in strength on μ-scale in schistosity direction or in any other direction seems to be a key factor. Not only does it influence the strength, but also the fracture pattern, and more importantly, the deformation behavior. Nasseri et al. (1997) made similar observations for rocks with a distinctive layered structure, namely quartzitic and chlorite schists. On the other hand, for quartz mica and biotite schists the fracture pattern resembled that of isotropic rock. The latter has a less pronounced layered structure and presumably no or a very small μ-scale strength difference between the different directions.

6 Conclusions

First, the use of digital visual recordings of the fracture process in slate makes it possible to determine fracture sequence and growth direction. This knowledge provides an insight in the different parameters that influence the strength and deformation behavior of slate. The results of AE-localization are in agreement with the visual observations and provide information on the interior of the sample.

Second, the series of loading tests of the circular samples shows that the strength on sample scale is dependent on the angle between the loading direction and the normal to the schistosity direction. The

identification of the different fracture types is a means to analyze and understand this strength anisotropy.

Third, it is suggested that the key factor is the difference in strength on μ-scale between schistosity direction and the other directions. Not only does this contribute in providing an explanation for the strength anisotropy, but also for the deformation behavior of slate on sample scale.

Fourth, the natural small variability in the schistosity direction as well as the occurrence of pyrite inclusions can visibly affect the fracture pattern in slate. In some cases this resulted in a complex 3D fracture pattern, rather than a composition of planar fractures.

References

Abad I, Nieto F, Gutiérrez-Alonso G (2003) Textural and chemical changes in slate-forming phyllosilicates across the external-internal zones transition in the low-grade metamorphic belt of the NW Iberian Variscan chain. Schweiz Mineral Petrogr Mitt 83:63–80

Al-Bazali TM, Zhang J, Chenevert ME, Sharma MM (2005) Measurement of the sealing capacity of shale cap-rocks. In: Proceedings of SPE annual technical conference and exhibition, SPE 96100

Andreev GE (1995) Brittle failure of rock materials: test results and constitutive-technology & engineering. Balkema, Rotterdam

Bombolakis EG (1968) Photo-elastic study of initial stages of brittle fracture in compression. Tectonophysics 6:461–473

Brady BHG, Brown ET (1993) Rock mechanics for underground mining, 2nd edn. Chapman and Hall, London

De Barquin F, Nicaise D (2005) Trial run on walloon stones in the framework of marking CE 2004–2005. WTCB report

Debecker B, Vervoort A (2009a) Numerical simulation of the fracture process in a transversly isotropic rock. In: Proceedings of the twelfth international conference on civil, structural and environmental engineering computing, Madeira, Portugal (in publication)

Debecker B, Vervoort A (2009b) Localization by acoustic emission in transversely isotropic slate. JAE (article submitted for publication)

Ewy RT, Cook NGW (1990) Deformation and fracture around cylindrical openings in rock—II. Initiation, growth and interaction of fractures. Int J Rock Mech Min Sci Geomech Abstr 27(5):409–427

Friedman M, Perkins RD, Green SJ (1970) Observation of brittle-deformation features at the maximum stress of Westerly granite and Solenhofen limestone. Int J Rock Mech Min Sci 7:297–306

Grosse CU, Reinhardt HW, Finck F (2003) Signal-based acoustic emission techniques in civil engineering. J Mat in Civ Eng 15(3):274–279

ISRM (1979) Suggested methods for determining the uniaxial compressive strength and deformability of rock materials. Int Soc Rock Mech Commun Stand Lab Field Tests; Int J Rock Mech Min Sci Geomech Abstr 16:135–140

Jaeger JC (1960) Shear failure of anisotropic rocks. Geol Mag 97:65–72

Jaeger JC, Cook NGW (1976) Fundamentals of rock mechanics. Chapman and Hall, London

Lomov SV, Willems A, Verpoest I, Zhu Y, Barburski M, Stoilova T (2006) Picture frame test of woven composite reinforcements with a full-field strain registration. Text Res J 76((3):243–252

Nasseri MH, Rao KS, Ramamurthy T (1997) Failure mechanism in Schistose Rocks. Int J Rock Mech Min Sci 34:3–4 (paper No. 219)

Sircar A (2004) Hydrocarbon production from fractured basement foundations. Curr Sci 87:147–151

Tavallali A, Debecker B, Vervoort A (2007) Evaluation of Brazilian tensile strength in transversely isotropic sandstone. In: Proceedings of the 11th congress of the international society for rock mechanics Lisbon, Portugal. Taylor & Francis Publications, pp 269–272

Van de Steen B, Vervoort A, Sahin K (2002) Influence of internal structure of crinoidal limestone on fracture paths. Eng Geol 67:109–125

Van de Steen B, Vervoort A, Napier JAL (2005) Observed and simulated fracture pattern in diametrically loaded discs of rock material. Int J Fract 131(1):35–52

Wawersik WR, Fairhurst C (1970) A study of brittle rock fracture in laboratory compression experiments. Int J Rock Mech Min Sci 7:561–575